Wind-Energy based Path Planning For Electric Unmanned Aerial Vehicles Using Markov Decision Processes

Wesam H. Al-Sabban[1,*] , Luis F. Gonzalez[1] , Ryan N. Smith[2], Gordon F. Wyeth[2]

***Abstract*— Exploiting wind-energy is one possible way to extend flight duration for Unmanned Arial Vehicles. Wind-energy can also be used to minimise energy consumption for a planned path. In this paper, we consider uncertain time-varying wind fields and plan a path through them. A Gaussian distribution is used to determine uncertainty in the Time-varying wind fields. We use Markov Decision Process to plan a path based upon the uncertainty of Gaussian distribution. Simulation results that compare the direct line of flight between start and target point and our planned path for energy consumption and time of travel are presented. The result is a robust path using the most visited cell while sampling the Gaussian distribution of the wind field in each cell.**

I. INTRODUCTION

Small, electric-powered, Unmanned Aerial Vehicles (UAVs) have been widely developed for use in both military and civilian applications [1]. Such aircraft can be used for many applications such as coastal or border surveillance, atmospheric and climate research, as well as remote environment, forestry, agricultural, and oceanic monitoring and imaging for the media and real-estate industries. However, one of the main limitations facing small UAV is their flight endurance regard to the limitations of the possible on board (fuel/battery) which can be carried by the UAV [2]. Significant energy can be obtained from the environment if the energy sources can be exploited wisely. Glider pilots and birds frequently use winds to improve range, endurance, or cross-country speed [3] [4].

There are three sources of wind energy available to exploit for this problem [5]:

1) Vertical air motion, such as thermal instabilities, orographic lift or wave.
2) Spatial wind gradients, such as horizontal shear layers.
3) Temporal gradients, causing horizontal gusts.

Although we can exploit all of these, difficulty arises due to the high variability in wind magnitude and direction. This is compounded by the difficulty to precisely forecast wind magnitude and direction and at multiple altitudes at different times. The magnitude and direction of the wind significantly affects the onboard power. Thus, optimal path planning considering variable and uncertain environmental conditions (horizontal wind, vertical wind) is a high importance for these vehicles to increase their efficiency by maximizing flight duration and minimizing power consumption. Converse to reducing power consumption, uncertain magnitude and direction of wind can actually cause uncontrollable forcing to be applied to the vehicle due to its small size. This can have catastrophical effects. Figure 1 illustrates the concept where a path to fly from starting point (step 1) to target point (step 5) through a wind field, exploiting wind energy is shown.

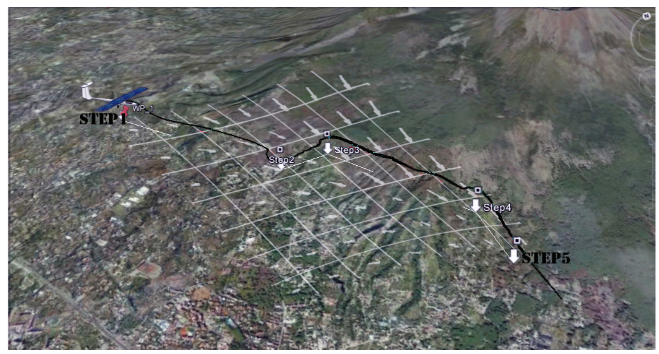

Fig. 1. A planned path that exploits wind energy from the start point (step1) to the target point (step5).

The concept of extracting energy from the environmental forces has been applied in many deferent types of robots, such as UAVs and Autonomous Underwater Vehicles (AUVs). Langelaan [6], [7] for instance presents an approach to plan long distance trajectories for small UAVs using orographic (i.e. slope) lift. The authors presented a tree-based approach, which uses a point mass model of the vehicle and knowledge of the wind field to generate feasible trajectories to a distant goal. Their work was limited to wind type and the change of the wind direction and magnitude with time and location. Chakrabarty and Langelaan [8] introduced a technique for long-range path planning for Small and Micro Unmanned Arial Vehicles called Energy Maps, which calculates the minimum total energy needed to reach the target point, from a starting point while accounting for the effect of wind fields. Their work did not consider the uncertainty of the wind field and the variation with respect to time. Chakrabarty and Langelaan [9] introduced an A* algorithm based on a cost function formed by the weighted sum of energy required and distance to goal. They compared the result of the required initial energy for varying weight with a wavefront expansion planning algorithm with the Energy Map approach introduced in [8]. In this work, they did not include variation of wind magnitude and direction with time.

Researchers have also used probabilistic path planning to solve the problem of uncertainty in the wind magnitude and direction. Wolf, *et al.* [10] introduced a probabilistic motion

*correspondent author : alsabban@student.qut.edu.au
[1] Australian Research Centre for Aerospace Automation, School of EECS, Queensland University of Technology, Brisbane,4001 QLD, Australia `www.QUT.edu.au`
[2] School of EECS, Queensland University of Technology, Brisbane,4001 QLD, Australia `www.QUT.edu.au`

planning algorithm in arbitrary, uncertain vector fields, with an emphasis on high-level planning for Montgolfiere balloons in the atmosphere of Saturn's Titan moon. The goal of the algorithm was to determine what altitude and what horizontal actuation, if any is available on the vehicle to use to reach a goal location in the fastest expected time. In this work, the authors integrate the uncertainty of the wind field into the wind model and use a Markov Decision Process (MDP) for planning. The authors proposed that because the wind velocity is uncertain, the next horizontal state may be considered a random variable, and a probability distribution can be constructed over all horizontally adjacent cells. Therefore, given these transition probabilities from all states the motion planning problem is then to select the actions (horizontal and vertical actuation of the balloon) that minimize time-to-goal. The MDP determines for each given current state, what is the optimal immediate action so that the expected cumulative time-to-goal is minimal. The authors applied the proposed technique on two cases: a stationary wind model, and a diurnally cyclical wind model.

Complementary to the research in UAVs, a similar problems have been approached for AUVs. The path planning can be proposed very similarly with winds being changed to currents. Garau, *et al.* [11] for example, used and adapted an A* algorithm to take current influence into account. The main disadvantages in their approach is that the variation of current with time not addressed. Kruger, *et al.* [12] introduced a continuous approach to energy optimal path planning where time is considered as an additional search dimension which allows the vehicle thrust to be chosen in an optimisation problem for minimal energy expenditure. The authors do not comment on the optimisation techniques to find the globally optimal path in complex environments. In [13] Witt and Dunbabin built upon the work by Kruger [12], and proposed optimisation swarms to aid in finding paths that are close to the global-minimum. The examples considered in [12] involved a rather simple artificial model of an estuary with static currents and obstacles, while in [13] the authors investigate more demanding planning cases in time-varying environments with dynamic obstacles using real ocean data. Rao and Williams [14] proposed a method for determining energy-optimal paths that account for the influence of ocean currents. The proposed technique is based on Rapidly-Exploring Random Trees (RRTs). The authors used forecasted ocean current data. They also compared the result of RRT method to grid based methods, and offer an improvement in terms of avoiding high-energy shallow regions.

In contrast to previous work, the proposed method offers the optimal power-based path, the path that minimises the onboard energy usage, taking into consideration the variation of wind magnitude and direction with time to reach a specific target point using Gaussian model and a modified MDP technique.

II. LATITUDINAL UAV DYNAMICS

We simplify the problim for this analysis by considering a planer problem of 3 DOF ,movement in the three dimensions but not rotation, for UAV, this will form a base for a path planner to extend into 6 DOF. The 3 DOF are represented by $x-position, y-position$, and the heading angle ψ. The altitude of the UAV $z-position$ will be constant in our study.

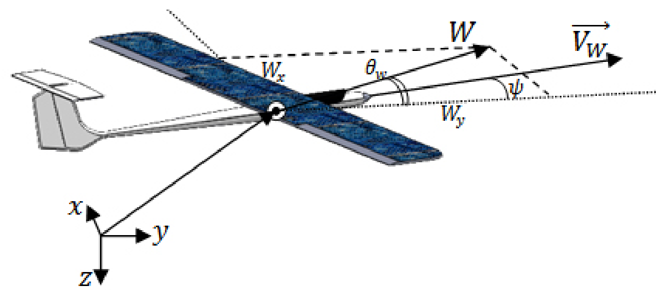

Fig. 2. Air-relative velocity and applied wind for a UAV.

Using the variable shown in Fig. (2) the equations are given by

$$\dot{X}_G = V_w \sin(\psi) + W_x, \tag{1}$$

$$\dot{Y}_G = V_w \cos(\psi) + W_y, \quad and \tag{2}$$

$$\dot{\psi} = \frac{V_w}{R_{min}}\ U \quad (-1 < U < 1) \tag{3}$$

By integrating Eq.(3)with respect to time, we get

$$\psi = \psi_0 + \frac{V_w}{R_{min}}\ U\ t. \tag{4}$$

Substituting Eq.(4) in Eq.(1) we get

$$\dot{X}_G = V_w \sin(\psi_0 + \frac{V_w}{R_{min}}\ U\ t) + W_x, \quad and \tag{5}$$

$$\begin{aligned} \dot{X}_G \quad = \quad & V_w[(\cos(\frac{V_w}{R_{min}}\ U\ t)\sin(\psi_0)) \\ & +(\cos(\frac{V_w}{R_{min}}\ Y\ t)\cos(\psi_0))U\ t) + W_x. \end{aligned} \tag{6}$$

By integrating Eq.(6) we get

$$X_G = \frac{-R_{min}}{U}\cos(\psi_0 + \frac{V_w}{R_{min}}\ U\ t) + W_x\ t\ + X_{G_0}. \tag{7}$$

Substituting Eq.(4) in Eq.(2) and by integrating the resulted equation we get

$$Y_G = \frac{R_{min}}{U}\sin(\psi_0 + \frac{V_w}{R_{min}}\ U\ t) + W_y\ t\ + Y_{G_0}. \tag{8}$$

Here $\dot{X}_G$ is the total velocity of the UAV in the x direction with respect to the ground, $\dot{Y}_G$ is the total velocity of the UAV in the y direction with respect to the ground, $\dot{\psi}$ is the angular velocity of the UAV, V_w is the UAV speed, R_{min} minimum turning radius of the UAV, W_x wind speed in x direction, and W_y wind speed in y direction. X_G and Y_G, and ψ represent x-coordinate, y-coordinate, and heading angle respectively which will identify the state of the UAV.

III. Path Planning

In this work a Markov Decision Process (MDP) is used to find the optimal wind-energy based path for a UAV in the presence of a wind field distribution which provide the best path to follow to minimise the onboard electric power consumption of the UAV. The motion-planning problem is to select the actions that minimise the power consumption of the UAV and minimise time-to-goal. This problem is thus naturally posed as a Markov Decision Process $(S; A; P; R)$, where: S denotes the set of possible states of the aircraft; A is the set of actions available from each state; P presents the transition probabilities $P_a(s_i; s_j)$ where (s_i) is the current state and (s_j) is the possible next states under action (a); R defines the expected immediate reward for each transition and each action (a).

A. MDP Problem Description

Given two points (Start and Target points) compute a path that minimises energy consumption by exploiting an uncertain, time-varying wind field for a UAV. The parameters of MDP are defined as:

Possible states (S): the number of possible states will be equal to the number of cells in the discretized grid. The Cartesian coordinates of the state of the UAV at the centre of a cell will be denoted by $S_{i,j} = x_{i,j}, y_{i,j}, \psi_{i,j}$ where $x_{i,j}, y_{i,j}, \psi_{i,j}$ denote x position, y position and heading angle for the UAV at cell$_{i,j}$ respectively. An important assumption is that the velocity of the aircraft is constant and equal to the Minimum Level-Flight Speed (V_{min}).

Actions available from each state (A): we assume that the UAV can move in eight directions, $A = N, NE, E, SE, S, SW, W, NW$ as shown in Fig. (3). where taking the action N means the heading angle (ψ) is equal to zero degree.

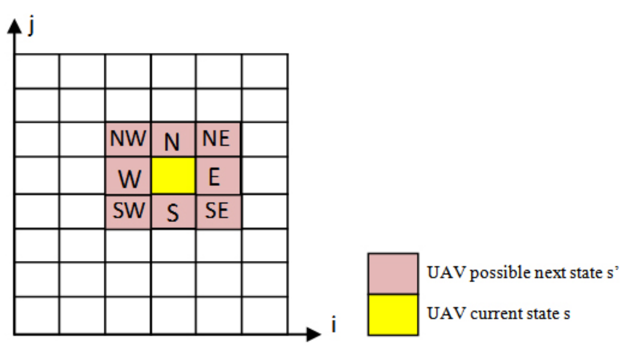

Fig. 3. A graphical representation of the eight possible end locations for the eight given actions of the UAV from a starting point in yellow and ending state in pink.

Transition probabilities (P): the transition probabilities $P : P_{s,a}(s, \grave{s})$ manage the probabilities of what state $\grave{s}$ is entered after executing each action A from state s. In this work we developed a method based on Gaussian distribution to assign a realistic transition probabilities $P_{s,a}$ in time varying wind field to fit inside the MDP framework.

The time-varying wind field is approximated by a Gaussian distribution, at each time step a vector is chosen from the distribution to find the direction and magnitude of the wind field. In simulation we considered both of uniform and non-uniform wind field. To determine the transition probabilities $P : P_{s,a}(s, \grave{s})$ the vector of the UAV velocity and the chosen vector of wind velocity at cell$_{i,j}$ are added. The summation result of the two vectors are represented by the magnitude $\overrightarrow{F}$ and direction ω using Eqs. (9,10,11).

$$F_x = V_{min} \cos(\psi_{i,j}) + W_{i,j} \cos(\theta_{i,j}), \tag{9}$$

$$F_y = V_{min} \sin(\psi_{i,j}) + W_{i,j} \sin(\theta_{i,j}), \quad and \tag{10}$$

$$\overrightarrow{F} = \sqrt{F_x^2 + F_y^2} \quad , \quad \omega = \tan^{-1}(\frac{F_y}{F_x}). \tag{11}$$

Figure 4 shows the normal distribution of transition probabilities (P) by setting ω from Eq. (11) as the mean value of a Gaussian distribution with standard deviation σ_ω in each cell. The Standard deviation will be selected by the user and is constant. The transition probabilities (P) will be represented by the area governed by the intersection between the curve and the range angle (Green line) for each state Eq. (12).

$$P : P_{s,a}(s, \grave{s}) = \frac{1}{\sigma\sqrt{2\pi}} \int_{\theta_a - \frac{\pi}{8}}^{\theta_a + \frac{\pi}{8}} e^{-\frac{1}{2}(\frac{\upsilon-\omega}{\sigma})^2} d\upsilon. \tag{12}$$

In this way we differentiate our work from previous work by considering planning of a path over time-varying wind field using an MDP planner.

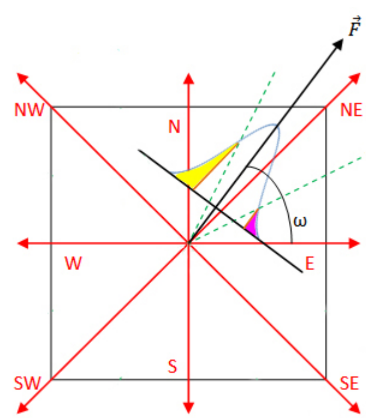

Fig. 4. The normal distribution of transition probabilities (P) by setting ω from Eq.(11) as the mean value of a Gaussian distribution with standard deviation σ_ω in each cell. In this example the total summation vector of the UAV velocity and wind velocity is represented by the black arrow, the probabilistic to reach the North state are shown by the yellow area, the probabilistic to reach the North-East state are shown by uncoloured area, the probabilistic to reach the East state are shown by the pink area.

Reward for each transition and each action (R): The direct reward value will be calculated based on the wind component facing the target cell Fig. (5). The ratio between the wind component facing the target point $(W_{i,j}\cos(\theta_{i,j}+\theta_T))$ and the maximum expected wind (W_{max}) value will be calculated and multiplying the result by a weight (C) - where (C) is selected by the user - using Eq. (13).

$$R_a(s_{i,j}) = (\frac{W_{i,j}\cos(\theta_{i,j}+\theta_T)}{W_{max}})C. \tag{13}$$

The value function $(V(s))$ for a cell will be equal to

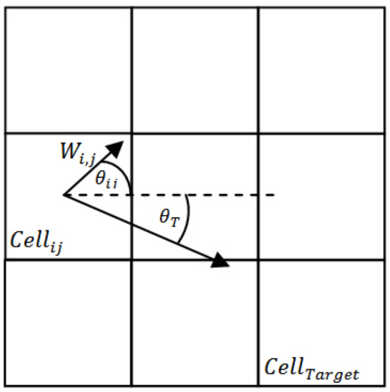

Fig. 5. Reward function

$$V(s_{i,j}) := E[R_a(s_{i,j}) + \gamma \sum (P_{s,a}(s,\grave{s})V(\grave{s})]. \tag{14}$$

The optimal value function $(V^*(s))$ for a cell will be given by

$$V(s_{i,j}) := max_a E[R_a(s_{i,j}) + \gamma \sum (P_{s,a}(s,\grave{s})V(\grave{s})], \tag{15}$$

where s is the initial state, $\grave{s}$ the next possible state, $R_a(s_{i,j})$ is the possible reward in state $s_{i,j}$ taken an action a, $P_{s,a}(s,\grave{s})$ is the probability of reaching $\grave{s}$ while applying action a in state $s_{i,j}$, and $V(\grave{s})$ is the value function for state $\grave{s}$.

It is important to notice that applying the previous equation Eq. (14) without using the discount factor γ may lead to the UAV not reaching the goal because the reward function is totaly dependent on the harvested power. Thus the factor γ which represent the time ratio $(1 > \gamma > 0)$ is added to the equation.

Identifying the optimal values $V^*(s)$ will lead to determine the optimal policy $\pi^*(s)$ using

$$\pi^*(s) = arg\ max_a(R_a(s_{i,j}) + \gamma \sum_{\grave{s}\in S}(P_{s,a}(s,\grave{s})V^*(\grave{s}). \tag{16}$$

Following the optimal policy will lead to the optimal path.

IV. SIMULATIONS AND RESULTS

We applied the above approach to three cases considering a time-variant wind field which depends on Gaussian distribution as explained in Section III-A. In the first case we will use a regular wind flow. The second case we will change the wind direction in the middle of the grid to see the behavior of the MDP path planner explained in Section III, the last case we will change the value of the wind magnitudes and directions by $(\zeta\ \sigma_w)$ and $(\zeta\ \sigma_\theta)$ where $(-1 \geq \zeta \leq 1)$ and (σ_w) is the standard deviation of the wind magnitude and (σ_θ) is the standard deviation of the wind direction to find all possible paths. In all these cases we will apply MDP value iteration.

A. MDP path and uniform wind flow

Case 1: We will use the mean value of the wind speed and direction in each cell as a single vector which represents the wind (W) as shown in Fig. (6). We will use minimum velocity of the aircraft as $V_{min} = 20$ m/s, maximum possible wind $W_{max} = 15$ m/s , and constant weight factor $C = 30$.

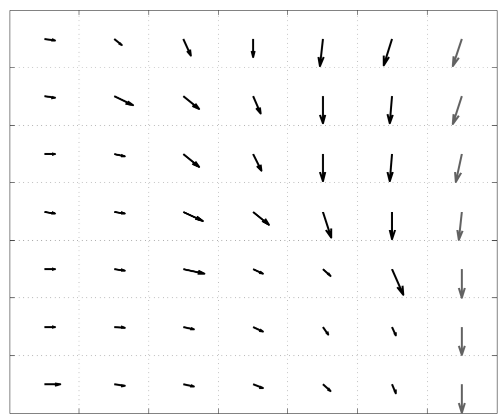

Fig. 6. Wind field distribution for Case 1, where the heads of arrows show the direction of the wind and the length of the arrows show the magnitude of the wind (5 - 15 m/s).

Figure 7 shows the optimal path. It can be seen that the MDP method does not produce a straight line between the starting cell and the target cell. The reason is that the method uses the wind field and MDP to find the highest gain cell to reach the target by using the minimum onboard energy.

B. MDP path and nonuniform wind flow

Case 2: We will use the mean value of the wind speed and direction in each cell as single vector which represents the wind (W,θ) as shown in Fig. (8). The main difference with the previous case is the change in the wind direction in the middle of the grid. The reason to do this test is to validate the algorithm and demonstrate how it will avoid an unwanted wind field distribution which leads to high power consumption or/and high drift from its path.

It can be seen in Fig. (9) that the MDP planner avoided an unwanted wind and find its way to the goal.

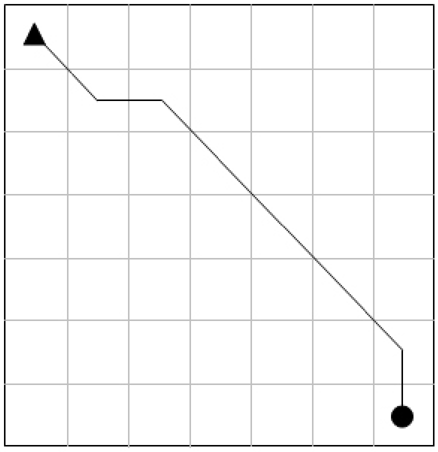

Fig. 7. MDP simulation result path for case 1. The triangle is the starting point, and the circle is the target point.

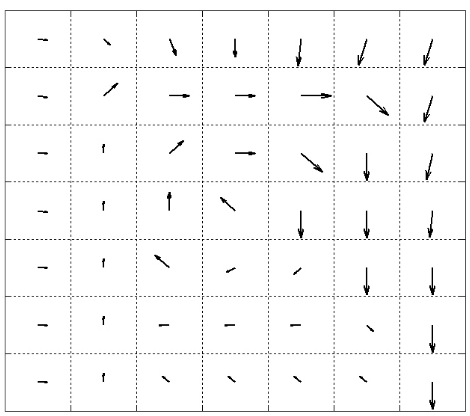

Fig. 8. Wind field distribution for case 2, where the head of arrows show the direction of the wind and the length of the arrows show the magnitude (5 - 15 m/s).

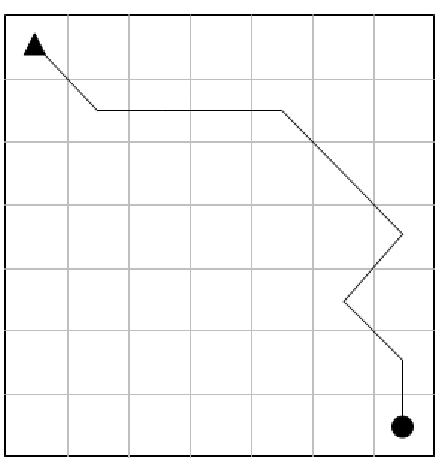

Fig. 9. Simulation resultant MDP path for Case 2, where the triangle is the starting point, and the circle is the target point.

C. MDP path for different wind standard deviation

Since the value function of the cells is based on a probability distribution rather than a single scalar value, we can produce not only the most-likely wind-energy path between two points on the map, but also sample from the wind probability distribution to produce a distribution of paths between the two points. Results are shown in the form of planned paths between the starting point and target point over the grid, these paths are shown to vary in response to local variations in value function Fig. (10).

Case 3: We use the same wind field distribution provided in case 1, however after finding the optimal path (which is the same as that shown in case one) the wind distribution is changed by (σ to $-\sigma$) with a 0.1 step increments. Then we compute the optimal path by choosing the most visited cell between the starting and the target cell to provide the optimal robust path because the probability of wind magnitude and direction at each cell in the grid contributes to identify the value function for each cell using MDP planner. This allows both the uncertainty in wind field and spatial variations in wind magnitude and direction to be incorporated into the planned path - red line- as shown in Fig. (10).

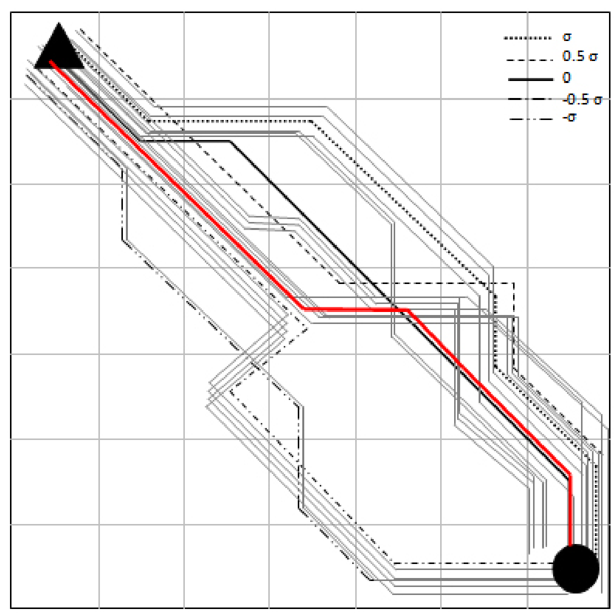

Fig. 10. Simulation resultant MDP path when the wind distribution is changed by (σ to $-\sigma$) with a 0.1 step increments.The red line is the most hit cell path.

D. Discussion

As seen in the previous three cases, the algorithm successfully reaches the target point in different wind field conditions. However, also want to knew if this path is the optimal path regarding the power consumption of the UAV. It is possible to compute the time required to reach the target point following the path generated by the algorithm and the direct straight line path between the starting and target points by taking into consideration the wind magnitude and direction in each cell and neglecting the possible drift of the aircraft caused by the wind. Assuming each cell is 1 km by 1 km wide we apply the wind field distribution and using values shown in Case 2 Fig. (8). Figure 11 shows the result, where the x-axis represents the time in minute, the y-axis represents the displacement in meters, the dashed line represents the MDP path, and the solid line represents the straight line path.

As shown in Fig. (11), the MDP path has a longer distance to reach the target point while the straight line has shorter distance, however the time required to reach the target point using the MDP path is less than the time required using the straight line path. Since the throttle of the aircraft is constant for all three cases the lower the time to reach the goal the lower the onboard power the aircraft will use to reach the goal. We can determine the efficiency of the MDP path as follows:

$$Eff_{path} = \frac{(T_{SL}) - (T_{MDP})}{(T_{SL})} \times 100, \tag{17}$$

where (Eff_{path}) represent the efficiency of the path, (T_{SL}) represent the time required to reach the goal using a straight line, and (T_{MDP}) represent the time required to reach the goal using MDP method. The efficiency of the MDP resultant path for Case 2 is therefor

$$Eff_{path} = \frac{(592.75) - (418.18)}{(592.75)} \times 100$$

$$Eff_{path} = 29.45\ \%$$

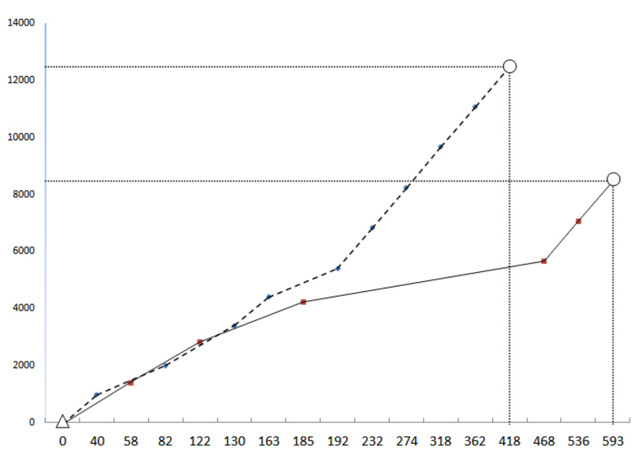

Fig. 11. Comparison between the time required to reach the target point using MDP path and straight line path between starting point and target point through wind field shown in case 2. The $x-axes$ represent the time, the $y-axis$ represent the displacement, the dashed line represent the MDP path plot, and the solid line represent the straight line path.

V. CONCLUSIONS

This paper presents a methodology for utilising an uncertain, time-varying wind field for a UAV using MDP. Simulated results demonstrate the validity of the planning for generating energy-paths in uncertain, time-varying wind fields. The use of a novel, hybrid Gaussian distribution of a wind field and the modified MDP technique with the velocity of the UAV to generate the probabilistic transition values provides not only an effective energy-path planning method which can effectively exploits the wind field, but also the robust path by using the most visited cells. Future work will extend the model to 6 DOF and include the cost of changing the heading angle of the UAV. Also it is an area of future work to extend and apply the proposed technique to AUV which can exploit ocean current energy.

REFERENCES

[1] J. Everaerts, "The use of unmanned aerial vehicles (uavs) for remote sensing and mapping," in *The International Archives of the Photogrammetry, Remote Sensing and Spatial Information Sciences*, vol. XXXVII, pp. 1187–1192, ISPRS Congress, 2008.

[2] A. J. Colozza, *Preliminary design of a long-endurance Mars aircraft*. NASA CR-185243, Washington, D.C.: National Aeronautics and Space Administration, 1990.

[3] M. J. Allen, "Updraft model for development of autonomous soaring uninhabited air vehicles," in *NASA Dryden Flight Research Center*, vol. 93523-0273, American Institute of Aeronautics and Astronautics, 2006.

[4] M. J. Allen and V. Lin, "Guidance and control of an autonomous soaring uav," Tech. Rep. NASATM2007214611, NASA Center for AeroSpace Information, 2007.

[5] J. W. Langelaan, "Biologically inspired flight techniques for small and micro unmanned aerial vehicles," in *Guidance, Navigation and Controls Conference*, vol. 2008-6511, American Institute of Aeronautics and Astronautics, 2008.

[6] J. W. Langelaan, "Long distance/duration trajectory optimization for small uavs," in *Guidance, Navigation and Control Conference*, vol. 2007-6737, American Institute of Aeronautics and Astronautics, 2007.

[7] J. W. Langelaan, "Tree-based trajectory planning to exploit atmospheric energy," in *American Control Conference*, pp. 2328 – 2333, 2008.

[8] A. Chakrabarty and J. W. Langelaan, "Energy maps for long-range path planning for small- and micro - uavs," in *Guidance, Navigation and Control Conference*, vol. 2009-6113, American Institute of Aeronautics and Astronautics, 2009.

[9] A. Chakrabarty and J. W. Langelaan, "Flight path planning for uav atmospheric energy harvesting using heuristic search," in *Guidance, Navigation, and Control Conference*, vol. 2010-8033, American Institute of Aeronautics and Astronautics, 2010.

[10] M. T. Wolf, L. Blackmore, Y. Kuwata, N. Fathpour, A. Elfes, and C. Newman, "Probabilistic motion planning of balloons in strong, uncertain wind fields," in *IEEE International Conference on Robotics and Automation*, pp. 1123 – 1129, 2010.

[11] B. Garau, A. Alvarez, and G. Oliver, "Path planning of autonomous underwater vehicles in current fields with complex spatial variability: an a* approach," in *IEEE International Conference on Robotics and Automation*, pp. 194–198, 2005.

[12] D. Kruger, R. Stolkin, A. Blum, and J. Briganti, "Optimal auv path planning for extended missions in complex, fast-flowing estuarine environments," in *IEEE International Conference on Robotics and Automation*, pp. 4265 – 4270, 2007.

[13] J. Witt and M. Dunbabin, "Go with the flow: Optimal auv path planning in coastal environments," in *Australian Conference on Robotics and Automation*, 2008.

[14] D. Rao and S. B. Williams, "Large-scale path planning for underwater gliders in ocean currents," in *Australasian Conference on Robotics and Automation*, 2009.